



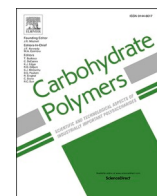
## **Role of intrinsic and extrinsic xylan in softwood kraft pulp fiber networks**

Downloaded from: <https://research.chalmers.se>, 2025-07-01 23:30 UTC

Citation for the original published paper (version of record):

Schaubeder, J., Spirk, S., Fliri, L. et al (2024). Role of intrinsic and extrinsic xylan in softwood kraft pulp fiber networks. Carbohydrate Polymers, 323. <http://dx.doi.org/10.1016/j.carbpol.2023.121371>

N.B. When citing this work, cite the original published paper.



# Role of intrinsic and extrinsic xylan in softwood kraft pulp fiber networks

Jana B. Schaubeder<sup>a</sup>, Stefan Spirk<sup>a</sup>, Lukas Fliri<sup>b</sup>, Eliott Orzan<sup>c</sup>, Veronika Biegler<sup>d</sup>,  
Chonnipa Palasingh<sup>b</sup>, Julian Selinger<sup>a,b</sup>, Adelheid Bakhshi<sup>a</sup>, Wolfgang Bauer<sup>a</sup>, Ulrich Hirn<sup>a,\*</sup>,  
Tiina Nypelö<sup>b,c,\*\*</sup>

<sup>a</sup> Institute of Bioproducts and Paper Technology, Graz University of Technology, Inffeldgasse 23, 8010 Graz, Austria

<sup>b</sup> Department of Bioproducts and Biosystems, Aalto University, Vuorimiehentie 1, FI-00076 Aalto, Finland

<sup>c</sup> Department of Chemistry and Chemical Engineering, Chalmers University of Technology, Kemivägen 10, 412 96 Gothenburg, Sweden

<sup>d</sup> Institute for Materials Chemistry and Research, University of Vienna, Währinger Straße 42, 1090 Vienna, Austria

## ARTICLE INFO

### Keywords:

Hemicelluloses

Paper

Enzymatic degradation

Adsorption

Mechanical properties

Bleached softwood kraft pulp

## ABSTRACT

Xylan is primarily found in the secondary cell wall of plants providing strength and integrity. To take advantage of the reinforcing effect of xylan in papermaking, it is crucial to understand its role in pulp fibers, as it undergoes substantial changes during pulping. However, the contributions of xylan that is added afterwards (extrinsic) and xylan present after pulping (intrinsic) remain largely unexplored. Here, we partially degraded xylan from refined bleached softwood kraft pulp (BSKP) and adsorbed xylan onto BSKP. Enzymatic degradation of 1 % xylan resulted in an open hand sheet structure, while adsorption of 3 % xylan created a denser fiber network. The mechanical properties improved with adsorbed xylan, but decreased more significantly after enzymatic treatment. We propose that the enhancement in mechanical properties by adsorbed extrinsic xylan is due to increased fiber-fiber bonds and sheet density, while the deterioration in mechanical properties of the enzyme treated pulp is caused by the opposite effect. These findings suggest that xylan is decisive for fiber network strength. However, intrinsic xylan is more critical, and the same properties cannot be achieved by readsorbing xylan onto the fibers. Therefore, pulping parameters should be selected to preserve intrinsic xylan within the fibers to maintain paper strength.

## 1. Introduction

Woody biomass contains 40–50 % cellulose, 25–35 % lignin, and 20–35 % hemicellulose (Bajwa et al., 2018). Plant hemicellulose consists primarily of xylan, which features a large structural variety depending on the plant species from which it is obtained. Both hardwood and softwood xylans consist of a backbone of  $\beta$ -1,4-linked D-xylose units with 4-O-methyl-glucuronic acid (MeGlcA) side groups (Ebringerová & Heinze, 2000; Shimizu, 1991). Hardwood xylans additionally contain O-acetyl groups, while softwood xylans contain 2-linked  $\alpha$ -L-arabinofuranosyl units (Ebringerová & Heinze, 2000; Pawar et al., 2013; Shimizu, 1991).

In the plant cell wall, the substitution pattern of these side groups closely correlates to the binding of xylan to cellulose microfibrils (Busse-Wicher et al., 2014; Wierzbicki et al., 2019). In hardwoods, the xylan regions, where the side groups are evenly spaced, interact with the

hydrophilic side of cellulose microfibrils via hydrogen bonding. The xylan regions of unevenly spaced side groups interact with the hydrophobic side of the cellulose microfibrils and act as a linker between these (Busse-Wicher et al., 2014; Wierzbicki et al., 2019). A distinct substitution pattern was also reported for the arabinosyl and MeGlcA side groups in softwood xylan, showing that xylan binds to the hydrophilic side of the cellulose microfibril (Busse-Wicher et al., 2016).

During chemical pulping and bleaching lignin is dissolved; yet cellulose and hemicellulose are also significantly modified and depolymerized. During alkaline cooking, xylan is partially dissolved in the early phase of cooking and is depolymerized by peeling reactions (Danielsson & Lindström, 2005). The rate of xylan dissolution depends on the amount of side chain substitutions; the fewer the substitutions, the more susceptible xylan is to peeling reactions. These reactions further accelerate the degradation of xylan during the cooking process. Only small amounts of xylan are redeposited onto the fiber surface

\* Corresponding author.

\*\* Correspondence to: T. Nypelö, Department of Bioproducts and Biosystems, Aalto University, Vuorimiehentie 1, FI-00076 Aalto, Finland.

E-mail addresses: [ulrich.hirn@tugraz.at](mailto:ulrich.hirn@tugraz.at) (U. Hirn), [tiina.nypelo@aalto.fi](mailto:tiina.nypelo@aalto.fi) (T. Nypelö).

<https://doi.org/10.1016/j.carbpol.2023.121371>

Received 29 April 2023; Received in revised form 31 August 2023; Accepted 6 September 2023

Available online 7 September 2023

0144-8617/© 2023 The Authors. Published by Elsevier Ltd. This is an open access article under the CC BY license (<http://creativecommons.org/licenses/by/4.0/>).

during pulping (Jacobs & Dahlman, 2001). In addition, during kraft pulping, the MeGlcA residues of xylan are mainly converted into 4-deoxyhex-4-enuronic acid (HexA) groups (Jacobs & Dahlman, 2001; Johansson & Samuelson, 1977). These HexA groups are then degraded during elemental chlorine free (ECF) bleaching, so that only about 12 % of the MeGlcA side groups remain after bleaching (Bergnor-Gidner, 1998; Buchert et al., 1995; Sjöberg et al., 2004). Apart from the degradation of the HexA groups during bleaching, the MeGlcA and arabinose side groups are relatively stable (Buchert et al., 1995).

After processing of wood to papermaking fibers, some xylan remains in the pulp fiber matrix, which contributes substantially to pulp quality and paper properties. Significant differences in paper properties become apparent depending on the fiber surface composition, such as xylan distribution and abundance, chemical composition, and molecular mass distribution (Henriksson & Gatenholm, 2002; Jacobs & Dahlman, 2001). Modification of pulp fibers via xylan adsorption and its effect on tensile strength, fiber-fiber bonding (Miletzky et al., 2015), wettability, hornification, and beatability have been intensively studied (Ban & Van Heiningen, 2011; Danielsson & Lindström, 2005; Han et al., 2012; Henriksson & Gatenholm, 2002; Kabel et al., 2007; Köhnke et al., 2010; Kontturi et al., 2021; Laine et al., 1997; Linder et al., 2003). In general, the adsorption of xylan enhances the mechanical strength of paper sheets, which has been attributed to a strengthening of the fiber-fiber joints due to two mechanisms. First, the increased swelling capacity of xylan, causing xylan to act like a glue (Pettersson & Rydholm, 1961; Rydholm, 1965). The pronounced tendency of xylan to swelling compared to cellulose microfibrils can be explained by the higher flexibility of xylan as well as by an increased surface charge due to the xylan side chain substitutions (Eriksson et al., 1991; Laine et al., 1997). Secondly, studies with xylan adsorption on cellulose thin films revealed that xylan is particularly effective in increasing the fiber-fiber bond strength in the presence of bivalent cations, i.e.  $\text{Ca}^{2+}$  (Rohm et al., 2014). Furthermore, xylan is affecting the paper network properties. As wetting increases, the flexibility of the fibers increases, which promotes conformability and leads to denser paper sheets with higher bonded area and thus higher tensile strength (Laine et al., 1997). This effect seems to be more pronounced with hardwood than with softwood fibers.

These findings suggest that swelling, flexibility and mechanical properties deteriorate as xylan is removed from the pulp fibers. To remove xylan without altering the cellulose matrix, xylanases can be employed. Xylanases selectively hydrolyze the 1,4- $\beta$ -D-xylosidic linkages of the xylan backbone under mild conditions. Despite the assumption that the access to xylan in pulp fibers is limited, these small enzymes (<30 kDa) have been found to act on both the surface and inner cell walls of pulp fibers (Paës et al., 2012; Suurnäkki et al., 1996). Although mechanical strength was expected to decrease after xylanase treatment, it was observed that strength properties remained unaffected, while the consumption of bleaching chemicals and energy for refining could be reduced (Bajpai et al., 1994; Garg et al., 1998; Przybysz Buzala et al., 2018; Rodell Lundgren et al., 1994; Roncero et al., 2003). Thus, the question of the effect of xylan on the strength properties of pulp fibers and the resulting hand sheets remains and there are only few studies (Schönberg et al., 2001) that directly compare the effects of adding and removing xylan from the same pulp.

In this work, we focus on the role of xylan in pulp fibers to elucidate the contribution of xylan to pulp and paper properties and the underlying mechanisms. The hypothesis was that the influence of xylan on hand sheet properties depends not only on the total xylan content and total fiber charge, but also on if the xylan is intrinsic to the pulp or extrinsic, that is, added afterwards. Therefore, we partially degrade xylan from refined ECF bleached softwood kraft pulp (BSKP) with an *endo*- $\beta$ -xylanase and adsorb beechwood xylan onto refined BSKP. A commercially available polymeric beechwood xylan with 11 % MeGlcA side chain substitution was chosen for the adsorption studies to increase the overall charge. However, differences in molecular mass and degree of substitution (amount of MeGlcA groups, HexA groups, and presence/

absence of arabinofuranosyl groups) of the remaining hemicelluloses in the BSKP are expected. Adsorption was performed under mild conditions compared to pulping to ensure that the composition and morphology of the cellulose fibers were not altered and that the resulting changes in material properties were solely attributable to the altered xylan. Xylan was degraded with a selective xylanase that did not affect the cellulose composition, as demonstrated by Przybysz Buzala et al. (2018). After characterizing the pulp (drainability, water retention value, fiber surface charge, fiber morphology), hand sheets were formed and surface topography, optical (brightness, color), barrier (air permeability), and mechanical (tensile properties, short-span compression strength, internal bond strength, zero-span tensile strength) properties were investigated. Our findings contribute to fill the knowledge gap of the role played by xylan in pulp fibers and enables to establish a strategy for delivering a target xylan composition and concentration in chemical pulp.

## 2. Experimental

### 2.1. Materials

Dried, ECF fully bleached softwood kraft pulp (BSKP; 85 % spruce, 10 % pine, 5 % larch) was kindly provided by Zellstoff Pöls AG (Austria) having ISO brightness of 88 % and a lignin content below 0.15 %. The degree of polymerization ( $\text{DP}_n$ ) of the BSKP was 3200 (intrinsic viscosity was determined according to ISO 5351 and converted to  $\text{DP}_V$  with the Mark-Houwink-Sakurada equation according to Kes and Christensen (2013)). Beechwood xylan with a 11 % glucuronic acid *O*-methyl substitution (monosaccharide composition xylose:glucuronic acid:other monosaccharides = 86.1:11.3:2.6, purity >95 %, molecular mass:  $M_n$  18.5 kDa,  $M_w$  23.8 kDa,  $M_w/M_n$  1.3) (Palasingh et al., 2022) and *endo*-1,4- $\beta$ -D-xylanase from *Neocallimastix patriciarum* (UNIPROT accession no. P29127; GH11) were purchased from Megazyme International (Ireland). Hydrogen peroxide ( $\text{H}_2\text{O}_2$ , 30 % in water) was purchased from Carl Roth, sulfuric acid ( $\text{H}_2\text{SO}_4$ ,  $\geq 95$  %) and sodium hydroxide (NaOH) were purchased from VWR Chemicals. Cationic (polydiallyldimethylammoniumchloride (polyDADMAC), 0.001 N,  $M_w$  107,000  $\text{g}\cdot\text{mol}^{-1}$ ) and anionic (polyanetholesulfonic acid sodium salt (PAT), 0.001 N,  $M_w$  9,000–11,000  $\text{g}\cdot\text{mol}^{-1}$ ) standard solutions for polyelectrolyte titration were purchased from BTG Instruments AB (Sweden). All above-mentioned chemicals were used as received.

### 2.2. Pulp refining

BSKP was soaked overnight in a 1:1 mixture of distilled water and tap water and then refined for 45 min in a valley beater according to ISO 5264-1. The refined pulp suspension, with a consistency of 1.57 % was directly proportioned into 8.3 L compartments for the subsequent experiments. Refining was carried out in two batches, the first batch being used for the whole xylan adsorption blank ( $\text{blank}_X$ ) and the whole xylan adsorption (X) experiments, and the second batch for the whole enzymatic degradation blank ( $\text{blank}_E$ ) and the whole enzymatic degradation (E) experiments.

### 2.3. Enzymatic degradation

The refined BSKP suspension (8.3 L, consistency 1.57 %) was poured into a vessel placed in a water bath. Temperature was adjusted to 50 °C and pH to 6 to provide optimal conditions for the enzyme. Once the conditions were met 1 mL of *endo*-xylanase stock solution (10,000  $\text{U}\cdot\text{mL}^{-1}$ ) was slowly added to the suspension and stirred at 190 rpm for 2 h. Then 8.8 mL  $\text{H}_2\text{O}_2$  (30 wt% in water) were added to deactivate the enzyme. After stirring thoroughly for 1 min, the pulp suspension was characterized and twelve hand sheets were formed. The blank experiment ( $\text{blank}_E$ ) was performed following the identical procedure just without addition of an enzyme.

## 2.4. Xylan adsorption

Beechwood xylan was swollen with 1 M NaOH overnight and dissolved in 1 M NaOH at a concentration of 50 mg·mL<sup>-1</sup> the next day. The refined BSKP (8.3 L, consistency 1.57 %) was poured into a vessel and pH was adjusted to 7 with 1 M H<sub>2</sub>SO<sub>4</sub>. The dissolved xylan was added to the suspension and then stirred thoroughly for 1 min. The pH was then adjusted to 7 with 1 M H<sub>2</sub>SO<sub>4</sub>. After stirring at 190 rpm for 2 h, the pulp suspension was characterized and twelve hand sheets were formed. The blank experiment (blank<sub>x</sub>) was performed equivalently to the xylan adsorption experiment by adding only 1 M NaOH (without xylan) to ensure that the resulting changes in pulp properties were not due to the treatment with alkali and acid.

## 2.5. Pulp characterization

### 2.5.1. Carbohydrate composition

Carbohydrate composition of all pulps was determined via hydrolysis in 72 % sulfuric acid according to Theander and Westerlund (1986) and monosaccharides were determined by using high performance anion exchange chromatography (HPAEC). This equipment uses a Dionex™ ICS-5000 ion chromatography system equipped with a CarboPac™ PA1 analytical column and an electrochemical detector, using NaOH and NaOH/NaOAc as eluents. Fucose was used as internal standard. The software used to analyze the peaks was Chromeleon™ 7, Chromatography Data System, v7.1.0.898. The quantified saccharides were corrected by hydrolysis yield (Wojtasz-Mucha et al., 2017).

### 2.5.2. NMR spectroscopy

The NMR spectra of the differently treated BSKP samples and of the commercially obtained xylan were recorded on a Bruker NMR AV III 400 spectrometer at an acquisition temperature of 65 °C. The materials were characterized by quantitative <sup>1</sup>H, diffusion-edited <sup>1</sup>H, and multiplicity-edited <sup>1</sup>H-<sup>13</sup>C HSQC experiments. The pulps were prepared in a [P<sub>4444</sub>][OAc]:DMSO-*d*<sub>6</sub> (1:4 wt%) electrolyte following published protocols (Fliri et al., 2023; King et al., 2018; Koso et al., 2020). In comparison to previous reports the measuring concentration of the pulps had to be reduced from 5 wt% to 2.5 wt%, in order to obtain solutions with suitable viscoelastic properties. This is a consequence of the high molecular mass of the pulp samples (DP<sub>n</sub>: 3200). The beechwood xylan was measured at a concentration of 5 wt%. Additionally, spectra in DMSO-*d*<sub>6</sub> were recorded, to assure the stability of the material in the used electrolyte. Chemical shifts are reported in parts per million (ppm) downfield relative to the residual proton of DMSO-*d*<sub>6</sub>. The obtained spectra are summarized in the Supplementary Information (Figs. S1-S18).

### 2.5.3. Total fiber surface charge

The total surface charge of the fibers was determined by poly-electrolyte titration using a Charge Analyzing System (AFG Analytic GmbH, Germany). The fibers (0.25 g dry mass) were immersed in 50 g 0.001 N cationic titrant (polyDADMAC, 107,000 g·mol<sup>-1</sup>) containing 0.01 M NaCl and stirred for 1.5 h. The solids (fibers and fines) were removed via repeated filtration through a very fine nylon sieve until the filtrate was clear and the filtrate was allowed to settle overnight. 10 mL of the filtrate was titrated with 0.001 N anionic titrant (PAT) until the streaming potential reached 0 mV. The titration rate was dynamically controlled at a maximum rate of 0.3 mL·min<sup>-1</sup>. In addition, 10 mL of 0.001 N cationic titrant was titrated with the anionic titrant to the neutral point to determine the blank value. Three titrations were performed per sample. The fiber surface charge *q* (mmol·kg<sup>-1</sup>) of the suspensions was calculated according to Eq. (1), where *V<sub>F</sub>* is the titration volume (mL) used for the fibers, *V<sub>b</sub>* is the titration volume (mL) used for the cationic titrant blank titration, *c* is the concentration of the titrant (mol·L<sup>-1</sup>), and *m* is the corresponding amount of dry mass of the pulp (g) (Bhardwaj et al., 2004). The total surface charge of the fibers is given as an absolute value of *q* and will be referred to as a surface charge.

$$q = \frac{(V_F - V_b) \cdot c \cdot 1000}{m} \quad (1)$$

### 2.5.4. Drainability, water retention value, and fiber characteristics

The drainability was determined according to the Schopper Riegler method (ISO 5267-1) measuring three samples and the water retention value was determined according to ISO 23714 measuring four samples. Fiber morphological characteristics of all pulp suspensions were determined using an L&W Fiber Tester Plus (ABB, Sweden) according to ISO 16065-2 by measuring >15,000 individual fibers per sample with three repetitions per sample.

## 2.6. Hand sheet preparation

All pulps were disintegrated (ISO 5263-1) and hand sheets were formed on a Rapid-Köthen sheet former (Frank PTI, Germany) using white water recirculation according to ISO 5269-2. Twelve hand sheets were formed per pulp with a basis weight of 80 g·m<sup>-2</sup>.

## 2.7. Hand sheet characterization

Prior to testing, all hand sheets were conditioned for at least 24 h in a climate room at 23 °C and 50 % relative humidity according to ISO 187. Thickness and apparent sheet density were determined according to ISO 534 with at least 14 measurement points. Optical properties of hand sheets such as opacity (C2), brightness and color (C2) were determined according to ISO 2471, ISO 2470-1, and ISO 5631-1, respectively, with 16 measurement points per analysis. Air permeability according to the Bendtsen method was measured according to ISO 5636-3 with at least 14 measurements. Tensile properties were determined according to ISO 1924-2 with a tensile tester (FRANK-PTI, Germany) with at least 14 measurements. Short-span compression (SCT) was determined according to ISO 9895, and Scott Bond internal bond strength was determined according to ISO 16260 with at least 14 measurements each. Zero-span tensile strength was determined according to ISO 15361 with a Z-Span™ 1000 (Pulmac, USA) measuring at least 14 samples each. Surface morphology of the fibers was determined by atomic force microscopy (AFM) using a FastScan Bio atomic force microscope (Bruker, USA) operated by a Nanoscope V controller. Antimony doped silicon cantilevers (RTESPA-150 from Bruker, USA) with a nominal spring constant and tip radius of 6 N·m<sup>-1</sup> and 8 nm, respectively, were used in tapping mode. Image processing was performed with Gwyddion v2.58 software. Scanning electron microscopy (SEM) images were recorded by means of a Sigma VP (Zeiss, Germany) in low-voltage mode (acceleration voltage: 0.7 kV) and detected with an in-lens detector and SE2 detector. The hand sheets were coated by sputter deposition with a 3.5 nm layer of iridium with an ACE600 sputter-coater (Leica Microsystems, Wetzlar, Germany).

## 3. Results and discussion

### 3.1. Chemical characterization

The chemical composition of the pulps was examined by carbohydrate analysis, solution state NMR spectroscopy and surface charge titrations, to investigate the influence of the different treatments on the xylan content and to connect it to changes in the materials properties. This represents a considerable analytical challenge, as the xylans in the focus of our study are only a minor component of the pulp fibers and the hand sheets and both the enzymatic degradation and the performed adsorption steps are not expected to drastically change the overall composition of the bulk material. Nonetheless, these small changes in composition, particularly on the fiber surface, can have a profound impact on the material properties.

The monosaccharide analysis of the pulps showed that both blanks



had a similar, yet not equal xylan content (blank after enzymatic degradation blank<sub>E</sub>: 9.6 % and blank of adsorption experiment blank<sub>X</sub>: 9.9 %). Thus, small amounts of xylan seem to be removed by dissolution during the treatments (Table S1). For the enzymatically treated pulp E (xylan content: 8.5 %), a degradation of approximately 1 % xylan was observed compared to blank<sub>E</sub>. For pulp X (xylan content: 12.9 %) where beechwood xylan was adsorbed, an increase in xylan content of 3 % was determined compared to blank<sub>X</sub>. Additionally, for all pulps mannoses were present in the hydrolysates. Thus, besides xylans, as expected, also glucomannans were present in the pulp, with contents ranging from 8.8 to 9.4 %. In contrast, the lignin contents were found to be insignificant and were excluded from the compositional analysis (Table S1).

To cross validate the data of the monosaccharide analyses and to investigate the side chain substitution in the xylans, the pulps were additionally examined by solution state NMR spectroscopy protocol using an ionic liquid ([P<sub>4444</sub>][OAc]) in DMSO-*d*<sub>6</sub> (1:4 wt%) as dissolving medium (Fliri et al., 2023; King et al., 2018; Koso et al., 2020). Owing to the high molecular mass of the pulp samples, a lower measuring concentration than reported in the original protocol had to be applied, resulting in a reduced signal to noise ratio. Furthermore, this led to broad peaks, which additionally superimposed with the hemicellulose signals. Instead, semi-quantitative and qualitative information could be obtained from the respective diffusion edited <sup>1</sup>H and <sup>1</sup>H-<sup>13</sup>C HSQC experiments. Comparison of the relative peak intensities of the anhydroglucose unit (AGU) C1-H at 4.40 ppm and anhydroxylose unit (AXU) C1-H at 4.20 ppm moieties in the diffusion edited <sup>1</sup>H spectra for the enzymatic degradation (blank<sub>E</sub> vs E; Fig. 1a) and the xylan adsorption (blank<sub>X</sub> vs X; Fig. 1b) experiments aligned with the changes in xylan content observed in the monosaccharide analysis. However, it must be considered that the intensities in the diffusion edited spectra are influenced by the molecular mass of the examined polymers (Fliri et al., 2023). The peak intensities of lower molecular mass constituents are heavily overestimated, which is evident in the similar peak heights of the AGU and AXU moieties in the spectra (Fig. 1). Thus, depolymerization reactions during the sample treatment might influence the peak ratios but those were not analyzed here. To investigate the adjacent side chains, the hemicellulose peaks in the pulps were compared with the commercially obtained beechwood xylan. As expected, no acetyl groups were present in the softwood xylans. The MeGlcA groups in the commercially obtained xylan showed two characteristic peaks for the C1-H moiety (<sup>1</sup>H: 4.78 ppm / <sup>13</sup>C: 98.3 ppm) and the methyl group (<sup>1</sup>H: 3.39 ppm / <sup>13</sup>C: 58.2 ppm) in the HSQC spectra, which did not overlap with other pulp constituents. Compared to values reported in a previous

NMR spectroscopic study on plant cell wall constituents (Cheng et al., 2013) the peaks were shifted to lower frequencies, especially in the <sup>1</sup>H dimension. Besides the differences in the employed dissolving media, presumably the higher measuring temperature of 65 °C used in this study (compared to 25 °C) influenced the shifts. In the pulp, no MeGlcA moieties could be detected. Only, the X sample featured MeGlcA signals referring to a small peak for the adjacent methyl group (<sup>1</sup>H: 3.39 ppm / <sup>13</sup>C: 58.2 ppm, see Fig. S18) in the HSQC and a minor signal in the diffusion edited <sup>1</sup>H spectra (<sup>1</sup>H: 4.78 ppm, see Fig. 1b). This indicates that, no substantial amounts of MeGlcA groups were present in the BSKP, otherwise they would have been visible in the NMR spectroscopy experiments. Contrary to what has been suggested in the literature (Jacobs & Dahlgren, 2001; Johansson & Samuelson, 1977), most of the MeGlcA groups in the BSKP were either cleaved off or converted to HexA groups during kraft pulping and subsequently cleaved off in the ECF bleaching process. Instead in the diffusion edited <sup>1</sup>H spectra of all pulps an additional peak at 5.24 ppm was present, with a weak coupling at 107.3 ppm in the HSQC experiments. This signal is in agreement with reported values of the C1-H moiety of arabinofuranosyl (Araf) side chains (Cheng et al., 2013). Furthermore, a peak at 4.57 ppm was visible, which can be assigned to the glucomannans present in the pulps (Holding et al., 2016).

Xylan is a negatively charged macromolecule as it carries carboxylic acid groups. Thus, the fiber surface charge of the pulps is expected to increase when such groups are added to the pulps. The surface charge of the pulps was similar for the blanks (Fig. 2a; Table S2). Adsorption of 3 % xylan increased the surface charge by 64 % (from blank<sub>X</sub>: 53 ± 5 mmol·kg<sup>-1</sup> to X: 87 ± 5 mmol·kg<sup>-1</sup>). In contrast, degradation of approx. 1 % xylan resulted in a decrease in surface charge of only 15 % (from blank<sub>E</sub>: 54 ± 6 mmol·kg<sup>-1</sup> to E: 46 ± 5 mmol·kg<sup>-1</sup>). This value agrees well with Schönberg et al. (2001), who determined a 7 % decrease in surface charge for a 0.5 % xylan degradation. The decrease in the surface charge in the enzyme treated pulp E is comparatively smaller than the increase in the xylan adsorbed sample X, which correlates with the NMR spectroscopy results, where no MeGlcA groups were detected in the BSKP, hence indicating that the intrinsic xylan in the BSKP is less charged than the pulp after (re)adsorption of xylan. Furthermore, the used xylanase requires three consecutive unsubstituted xylose units to cleave the xylan backbone one linkage before the MeGlcA-substituted xylose unit (Biely et al., 2016; Paës et al., 2012). Assuming that there are only a few MeGlcA substitutions left in the BSKP xylan (below the detection limit of NMR spectroscopy), enzymatic degradation would result in shortening of some xylan chains but only minor degradation of

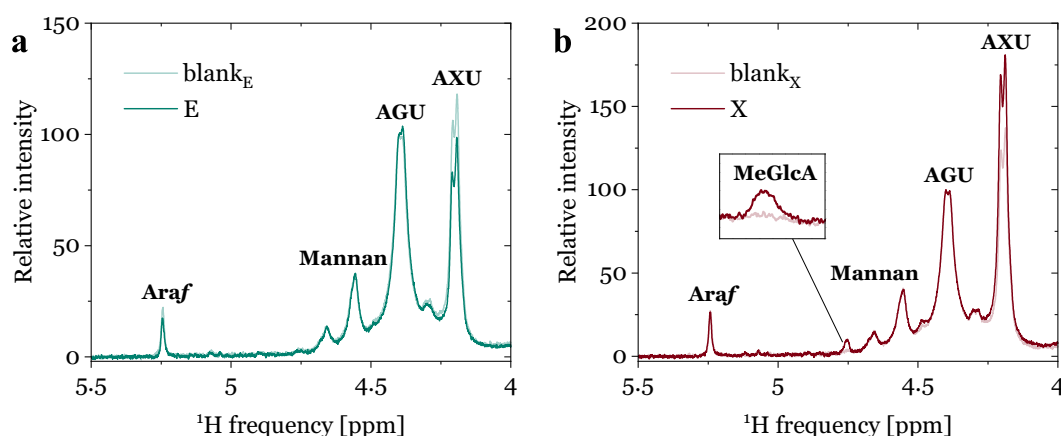


**Fig. 1.** NMR spectroscopy showing diffusion edited <sup>1</sup>H spectra with a zoom into the characteristic C1-H spectral area ([P<sub>4444</sub>][OAc]:DMSO-*d*<sub>6</sub>, 1:4 wt%; 400 MHz; 65 °C) for the enzymatic degradation and xylan adsorption experiments. a) Comparison of blank<sub>E</sub> with E shows a relative reduction of the AXU intensity as expected for the enzymatic treatment. b) After the performed xylan adsorption, the relative peak intensity of the AXU moiety increases from blank<sub>X</sub> to X. All spectra referenced and normalized to the C1—H resonance of the AGU moiety (4.40 ppm). Peak assignments based on comparison with the spectra from commercial beechwood xylan or with literature values (Cheng et al., 2013; Holding et al., 2016). The minor unassigned peaks are either caused by other hemicellulose components or branched AXU moieties. With the used experimental setup, it was not possible to further assign them.

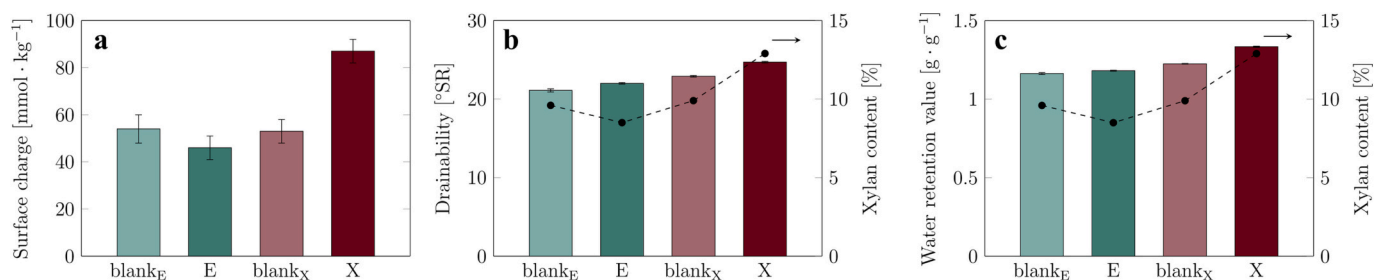


**Fig. 2.** a) Surface charge of all pulps, determined by polyelectrolyte titration, shows a 64 % increase for X and only a 15 % decrease for E. b) Drainability according to the Schopper-Riegler method is reduced for X. c) Water retention value shows an 8 % increase for X.

xylan, consistent with the decrease in xylan content of about 1 %. The term intrinsic xylan refers to xylan originally derived from the wood from which the pulp was made, meaning that the xylan has already undergone changes in chemical composition and specific location depending on the relevant pulping conditions. In contrast, extrinsic xylan refers to xylan added after pulping.

### 3.2. Drainability is reduced while WRV increases for xylan adsorbed pulp

The BSKP was refined prior to the treatments to achieve a larger surface area that facilitates enzyme access and increases the surface area for xylan adsorption. The drainability expressed as Schopper Riegler number [SR] with higher SR values indicating a reduced drainability, was  $21.1 \pm 0.2$  °SR for blank<sub>E</sub> and  $22.9 \pm 0.1$  °SR for blank<sub>X</sub> (Fig. 2b). This difference in drainability can be explained by the fact that they were refined in a different batch and slight variations between batches were to be expected. The dewatering ability is slightly reduced for the xylan adsorbed pulp (from  $22.9 \pm 0.1$  °SR for blank<sub>X</sub> to  $24.7 \pm 0.1$  °SR for X), which was also the case in the literature (Silva et al., 2015). Overall, however, the pulp treatments appeared to have little effect on drainability. Water retention values (WRVs) were similar for all pulps (blank<sub>E</sub>:  $1.16 \text{ g} \cdot \text{g}^{-1}$ , E:  $1.18 \text{ g} \cdot \text{g}^{-1}$ , and blank<sub>X</sub>:  $1.23 \text{ g} \cdot \text{g}^{-1}$ ), except for X, where a higher value of  $1.33 \text{ g}$  water per  $\text{g}$  pulp was obtained, corresponding to an increase of 8 % for X compared to blank<sub>X</sub> (Fig. 2c). This indicates that the xylan-containing pulps have a higher water retention capacity, stemming from their higher swelling capacity, which is widely accepted in literature (Eriksson et al., 1991; Han et al., 2012; Pettersson & Rydholm, 1961; Rydholm, 1965). However, in pulp E, the WRV did not decrease with the degradation of about 1 % of xylan, which was also the case in the literature (Schönberg et al., 2001). It can be speculated that the xylan removed from the fiber wall is leaving behind pores that can be filled with water, thus preserving the water retention capacity.

### 3.3. Fiber morphology remained unchanged

Furthermore, the fiber morphology was investigated. The weight-weighted mean values of the fiber properties were used because the plain mean values are mainly reflecting the number of fine particles in the pulp instead of describing the fiber properties, hence the weight-weighted mean values also correspond best to the sheet properties (Pulkkinen et al., 2006) (Table S3). Length and width of the pulp fibers were essentially equivalent, ranging from 3.21 to 3.25 mm and 32.9 to 33.1 μm, respectively. The fines content varied somewhat and was highest for the X fibers and lowest for the blank<sub>E</sub> fibers, which is in agreement with the measured drainability values. The weight-weighted fiber distributions of all pulps show no clear differences among them (Fig. S19). Coarseness, which is a measure of the change in fiber mass per unit length, is an important pulp property for dewatering, optical properties and strength of the dry paper sheets (Pulkkinen et al., 2006). Similar values were obtained for the coarseness of the fibers, which ranged from 133 to 137 μg · m<sup>-1</sup> (Table S3). Curl, mean-kink-angle, and fibril area gave comparable values for all pulp fibers with only slightly

increased values for X (Table S3). In summary, addition and removal of xylan – as expected – did not change the fiber morphology.

### 3.4. Enzymatic treatment exposes the fibrils and creates a less dense fiber network

Even though no significant differences in the paper technical properties were determined for the individual fibers of all pulps, a closer look was taken at the fiber surface topography by AFM. Images Fig. 3a-d provide a qualitative indication of the structural differences after xylan degradation and xylan adsorption, and were selected as representative of the respective fiber surface (see Fig. S20 for a summary of the images acquired). Looking at the surface morphology of E, the fibrils appear to be less embedded in the fiber matrix and more exposed, which could be due to surface xylan degradation or preferential cleavage of the xylan domains between individual cellulose fibrils. No major differences in surface morphology were observed in the blank samples (blank<sub>E</sub> and blank<sub>X</sub>) and X by AFM. However, investigating pulp fibers by AFM presents some challenges, such as the anisotropic properties and roughness of the fiber surface, which can lead to artifacts or distortions on the images. Therefore, we also acquired SEM images of fiber-fiber-transitions and the fiber surface (Fig. 3e-l, Figs. S21, S22). The fiber network, which in the context of this work corresponds to the network of the hand sheets, appears overall smoother in E (Fig. S21d) than in blank<sub>E</sub> (Fig. S21b). This smoothing effect results from a higher proportion of fibrils on the surface, which only become visible at higher magnification. In addition, at a magnification of 1 kx (Fig. 3e,f), the pits show only a slight distortion in blank<sub>E</sub>, whereas they appear frayed in E, indicating partial degradation by the enzyme. At higher magnifications of 20 and 50 kx (Fig. 3i,j and Fig. S22a,b), the fibrils appear likewise more prominent in E than in blank<sub>E</sub>.

When looking at the fiber network of blank<sub>X</sub> (Fig. S21e,f) and X (Fig. S21g,h) at a low magnification, no clear differences are apparent. The mechanism of xylan adsorption onto cellulose fibers was proposed already in the early 2000s showing that xylan is partially aggregating in aqueous solutions. These pre-formed aggregates then adsorb to the cellulose surface by interactions between the unsubstituted, linear regions of the xylan chains (Henriksson & Gatenholm, 2001; Linder et al., 2003; Linder & Gatenholm, 2003; Qaseem & Wu, 2020). Only at a higher resolution of 20 kx (Fig. 3l) these aggregates become visible on the fiber surface, confirming that the adsorption of xylan occurred likely onto the fiber surface.

### 3.5. Xylan adsorption increased the sheet density, while enzymatic degradation led to a decrease in sheet density

The hand sheets had similar thicknesses of 122 to 128 μm with slight variations in density (Fig. S23a; Fig. 4a, Table S4). The density decreased by 1.7 % from  $0.642 \pm 0.005 \text{ g} \cdot \text{cm}^{-3}$  for blank<sub>E</sub> to  $0.631 \pm 0.003 \text{ g} \cdot \text{cm}^{-3}$  for E and increased by 2.0 % from  $0.642 \pm 0.003 \text{ g} \cdot \text{cm}^{-3}$  for blank<sub>X</sub> to  $0.655 \pm 0.004 \text{ g} \cdot \text{cm}^{-3}$  for X. This 2 % increase in sheet density for X indicates that the addition of xylan results in a denser

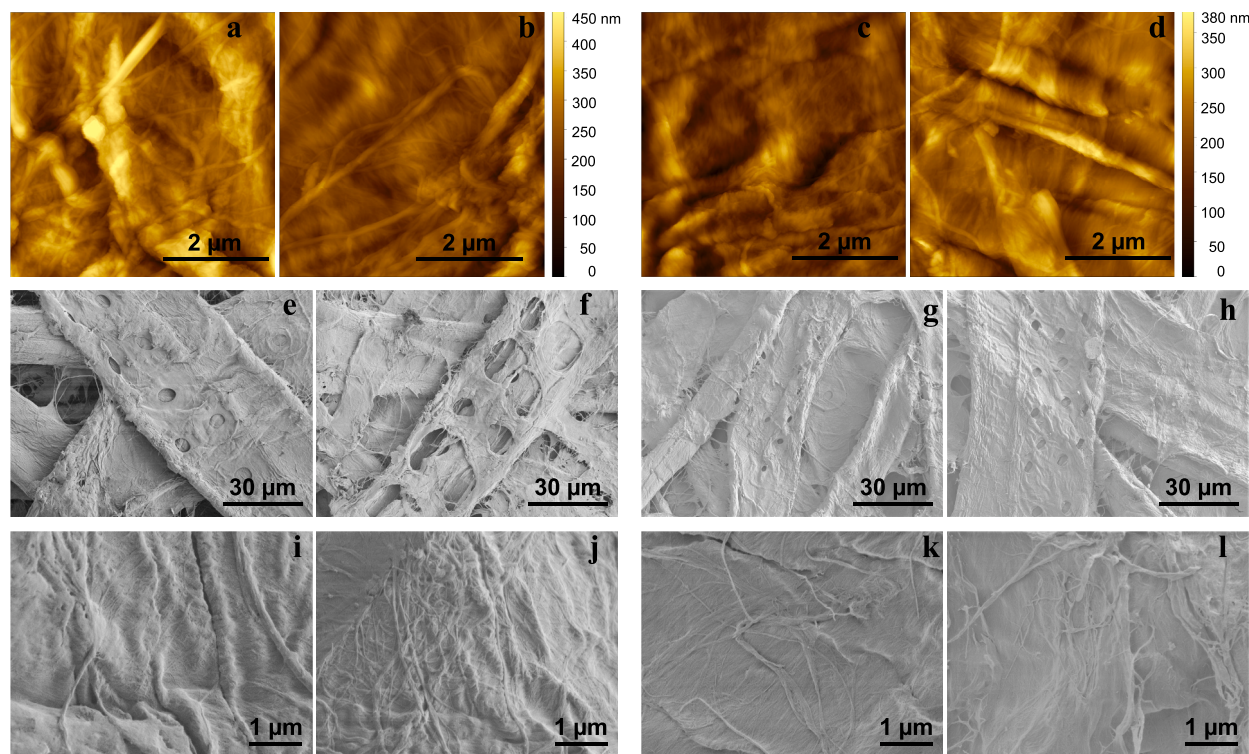


**Fig. 3.** AFM height images (5 × 5 μm<sup>2</sup>) of a) blank<sub>E</sub>, b) E, c) blank<sub>X</sub>, and d) X show more exposed fibrils for E. SEM images with a magnification of e-h) 1 kx and i-l) 20 kx of blank<sub>E</sub> (e and i), E (f and j), blank<sub>X</sub> (g and k), and X (h and l) recorded with a signal overlay from in-lens detector and SE2 detector (ratio: 45/55) showing a higher share of fibrils in E and adsorbed xylan aggregates for X.

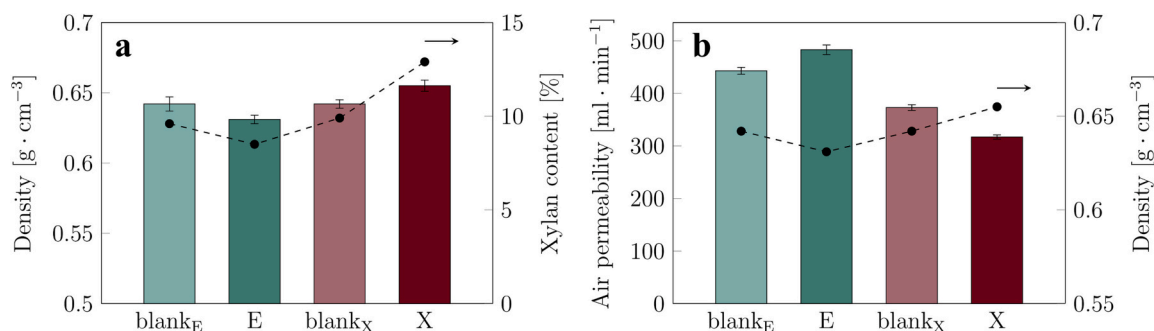


**Fig. 4.** a) Density of all hand sheets decreases by 1.7 % for E and increases by 2 % for X. b) Air permeability according to the Bendtsen method increases by 9 % for E and decreases by 15 % for X.

bonding of the fibers, as suggested by Laine et al. (1997). Moreover, the decrease in sheet density for E with a constant fiber morphology indicates that the fibers become stiffer when xylan is removed. Further, a 2 % increase as well as a 1.7 % decrease in density can have substantial effects on the air permeability and the mechanical properties of the hand sheets. An increase in sheet density can also be achieved by increasing the fines content through refining, which in turn increases paper strength through better bonding (Mandez et al., 2022; Motamedian et al., 2019). However, the fines content of our pulps does not vary substantially, so the density change can be attributed to the xylan.

To better understand the porosity of the fiber network structure, the air permeability was explored. Significant differences in air permeability were determined (Fig. 4b; Table S4), even for the blank samples, with the air permeability of blank<sub>E</sub> (443 ± 7 mL·min<sup>-1</sup>) being higher than that of blank<sub>X</sub> (373 ± 5 mL·min<sup>-1</sup>). Air permeability generally correlates well with the sheet density, and hence, the 9 % increase in air permeability for E (to 443 mL·min<sup>-1</sup>) can be explained by a decrease in paper density. In contrast, a decrease in air permeability of 15 % (to 317

mL·min<sup>-1</sup>) was observed for X, which probably results from the 2 % increase in paper density. In literature, no change in air permeability was observed with hemicellulose adsorption to BSKP (Hu et al., 2016). However, we cannot explain the difference in air permeability of the blanks because it is not due to differences in formation (flocculation), density, fiber morphology, or fibrillation.

### 3.6. Optical properties show a shift towards yellow for xylan adsorbed hand sheets

As established above, the adsorbed xylan is located in the outer layers of the fibers, where it should contribute more to the optical properties such as reflection. Thus, an influence on the optical properties is expected. Indeed, X showed a decrease in brightness of 4.3 % (to 83 %), while E showed even a slightly increased brightness (88.5 %) compared to the blanks (blank<sub>E</sub>: 87.9 % and blank<sub>X</sub>: 86.7 %) (Fig. 5a). Thus, adsorption of xylan onto pulp results in a less bright paper that reflects less blue light. The increase in xylan content for X goes hand in



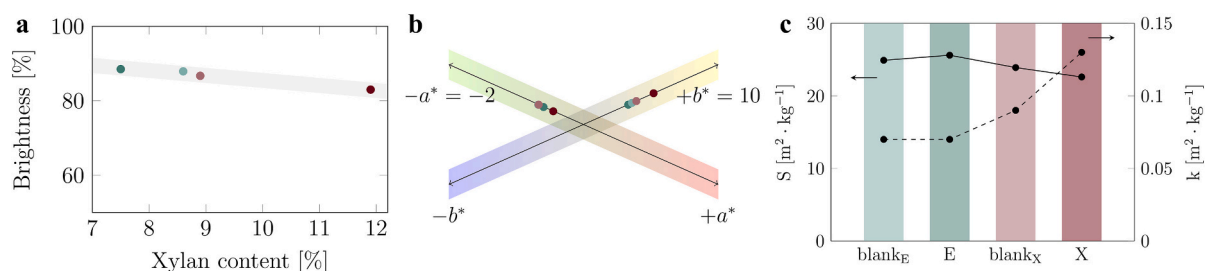


**Fig. 5.** a) Brightness (standard error of mean < 0.2 %) for blank<sub>E</sub> (light-blue), E (blue), blank<sub>X</sub> (light-red), and X (red) show a clear trend towards lower brightness with increasing xylan content. b) a\*b\* color space shows a color shift towards yellow for X (red). c) Light scattering coefficient S (left) and absorption coefficient k (right) show structural changes for E and X and a color change for X.

hand with an increase in the surface charge, which has been found to participate in brightness reversion (Buchert et al., 1997). The color of the hand sheets is represented in the L\*a\*b\* color space, where L\* corresponds to the lightness, a\* to the color range from green (negative values) to red (positive values), and b\* to the color range from blue (negative values) to yellow (positive values) (Fig. 5b). We are not considering lightness here for clarity. All hand sheets showed a slight color shift towards green, which was less pronounced for X, and all hand sheets showed a distinct shift towards yellow, which was more pronounced for X (Table S4). To determine whether this color shift is due to a structural change or to the light absorption, so the color of xylan itself, the light scattering coefficient S and the absorption coefficient k were evaluated (Fig. 5c, Table S4). The scattering coefficient increased for E (from 24.9 m<sup>2</sup>·kg<sup>-1</sup> (blank<sub>E</sub>) to 25.6 m<sup>2</sup>·kg<sup>-1</sup>) and decreased for X (from 23.9 m<sup>2</sup>·kg<sup>-1</sup> (blank<sub>X</sub>) to 22.6 m<sup>2</sup>·kg<sup>-1</sup>), which can be correlated with the density changes for E and X and indicate an increase in fiber-fiber contact area. The absorption coefficient k can be correlated with a color change and does not change from blank<sub>E</sub> (0.07 m<sup>2</sup>·kg<sup>-1</sup>) to E (0.07 m<sup>2</sup>·kg<sup>-1</sup>), while it increases from blank<sub>X</sub> (0.09 m<sup>2</sup>·kg<sup>-1</sup>) to X (0.13 m<sup>2</sup>·kg<sup>-1</sup>). These results show that the adsorption of xylan is accompanied by a color shift towards yellow resulting from a combined effect of a change in color absorption of xylan itself and structural changes in the

paper sheets, while degradation of xylan from an already bleached pulp shows a slight shift towards blue resulting from solely structural changes in the paper sheets. Furthermore, if we look at the relative changes of blank<sub>E</sub> to E and blank<sub>X</sub> to X, the effect of xylan adsorption is much stronger than that of xylan degradation. Combined with the decline in whiteness for X (Table S4) the xylan is indeed located at the outer layers of the fiber.

### 3.7. The internal bond strength correlates well with xylan content

The internal bond strength provides information on the bonding strength between the fibers. The determined internal bond strength correlates well with the xylan content (Fig. 6a; Table S5). The internal bond strength decreased by 11.9 % with decreasing xylan content (from blank<sub>E</sub>: 53.8 ± 0.3 J·m<sup>-2</sup> to E: 47.4 ± 0.4 J·m<sup>-2</sup>) and increased by 15.9 % with increasing xylan content (from blank<sub>X</sub>: 59.1 ± 0.5 J·m<sup>-2</sup> to X: 68.5 ± 0.4 J·m<sup>-2</sup>). The internal bond strength for blank<sub>X</sub> was slightly higher than for blank<sub>E</sub>, which could be influenced by the different experimental procedures. Schönberg et al. (2001) presented a correlation of internal bond strength with the xylan content showing a decrease in internal bond strength of 23 % for a xylan degradation of 0.9 % and an increase of 22 % for a xylan adsorption of 1.5 %. The effect of xylan on

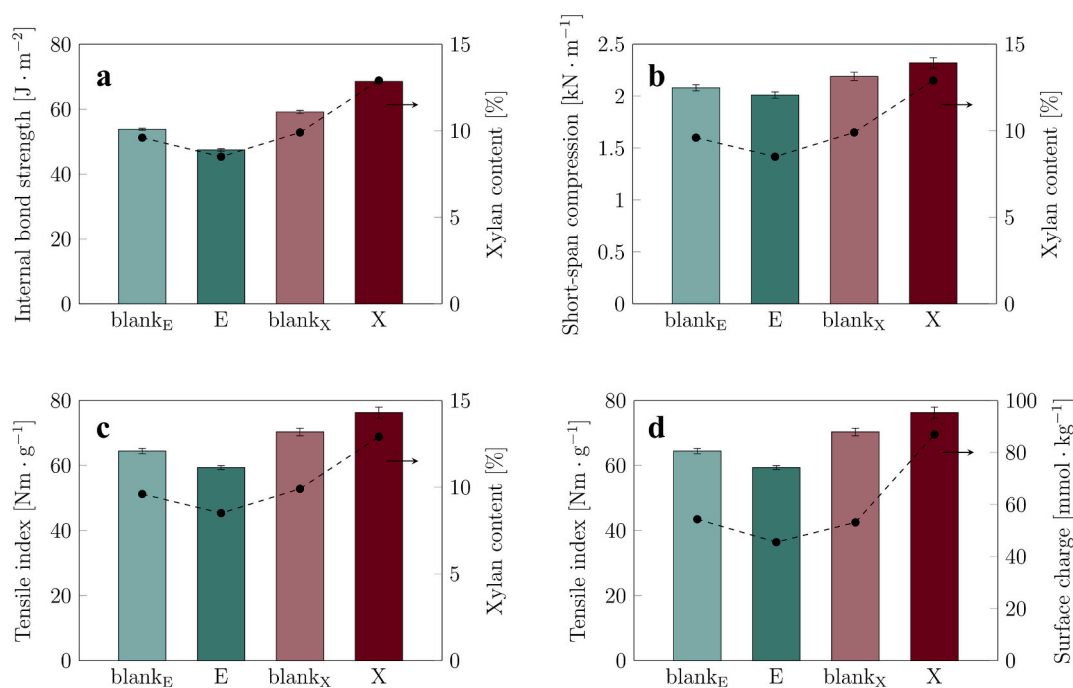


**Fig. 6.** a) Internal bond strength of all samples in correlation with xylan content, showing a good correlation between internal bond strength and xylan content. b) Short-span compression strength. Correlation of tensile index of all samples with c) xylan content and d) surface charge, showing a correlation with xylan content and a minor correlation with surface charge.



fiber bond strength described in literature thus has also been found in our investigations. It is, however, interesting that the removal of about 1 % of xylan is decreasing the bond strength to a similar extent as the addition of 3 % xylan. It may be speculated that the adsorbed, extrinsic xylan forms aggregates and thus is less effective in increasing bonding strength than the xylan intrinsically present in the fibers.

### 3.8. Short-span compression strength shows the same behavior as tensile properties

The short-span compression test (SCT) showed a similar trend as tensile properties (Fig. 6b; Table S5). SCT decreased by 3.4 % from blank<sub>E</sub> ( $2.08 \pm 0.03 \text{ kN}\cdot\text{m}^{-1}$ ) to E ( $2.01 \pm 0.03 \text{ kN}\cdot\text{m}^{-1}$ ) and increased by 5.9 % from blank<sub>X</sub> ( $2.19 \pm 0.04 \text{ kN}\cdot\text{m}^{-1}$ ) to X ( $2.32 \pm 0.05 \text{ kN}\cdot\text{m}^{-1}$ ). Again, a better correlation with xylan content than with surface charge was obtained. However, the increase in SCT value was again lower than expected for the 3 % xylan adsorption for X. This compressive strength of paper correlates well with the tensile properties, which can be explained by the change in density. It can be suspected that also the increase in bond strength is further improving the compressive strength. However, it needs to be mentioned that the increase in SCT value for X is not assumed to be due to stiffer fibers. On the contrary, as shown above, the fibers are getting softer with adsorbed xylan as evidenced by the increase in sheet density.

### 3.9. Tensile properties deteriorate with xylan removal by enzyme, while xylan adsorption leads to only a marginal improvement

Tensile properties were investigated as one of the main criteria for the mechanical performance of paper sheets. Tensile index, which is the tensile strength divided by grammage, decreased significantly by 8.0 % for E (from blank<sub>E</sub>:  $64.4 \pm 0.8 \text{ Nm}\cdot\text{g}^{-1}$  to E:  $59.3 \pm 0.6 \text{ Nm}\cdot\text{g}^{-1}$ ), while an 8.5 % increase was observed for X (from blank<sub>X</sub>:  $70.3 \pm 1.2 \text{ Nm}\cdot\text{g}^{-1}$  to X:  $76.3 \pm 1.7 \text{ Nm}\cdot\text{g}^{-1}$ ) (Fig. 6c,d; Table S5). It has been suggested that the tensile properties correlate with the amount of surface hemicellulose content (Sjöberg et al., 2004) and especially with the total fiber charge (Laine et al., 1997; Schönberg et al., 2001), which is also the case for the pulps that were investigated here (Fig. 6d). Furthermore, a correlation with the xylan content is shown, but an even higher tensile index for X would have been expected according to the 3 % increase in xylan content (Fig. 6c). The same trend was found for all tensile measurements (Table S5) such as the tensile energy absorption (TEA) index (Fig. S24a) and Young's modulus (Fig. S24b). TEA index, which shows the papers ability to absorb energy and thus its durability or resistance to repeated stress or strain, decreased by 8.4 % for E while it increases by only 2.9 % for X. Young's modulus, which shows the elastic deformation under load that is recoverable, with high values corresponding to stiff materials and low values to elastic materials, shows a 4 % decrease for E, but a 7.7 % increase for X. These results suggest that the enzymatic treatment deteriorate the tensile properties of the papers, even though only about 1 % xylan was degraded, while a 3 % xylan adsorption in comparison lead to an improvement, which was similar in absolute numbers, but lower in relation to the xylan amount added. This would agree with the assumption that the aggregated extrinsic xylan does not contribute as much to the mechanical properties as the intrinsic xylan. In addition, the blank samples show some variation, indicating that the treatments themselves have already influenced the tensile properties of the pulp. Furthermore, the paper density is decisive for tensile strength. Mandlez et al. (2022) reported that an increase in density of only 2 % can lead to an increase in tensile strength of about 5 to 8 % as well as a decrease in sheet density consequently leads to a decrease in tensile strength. An increase in internal bond strength is also beneficial for the tensile strength and should lead to its increase.

To show that fiber network failure at the refining level used in this work does not depend on the fiber strength itself, but rather on the fiber-fiber bond strength, zero-span tensile strength was determined, which

showed no significant differences for all pulps and ranged from  $11.2 \pm 0.7$  to  $12.2 \pm 1.0 \text{ kN}\cdot\text{m}^{-1}$  (Table S5, Fig. S24c). The internal bond strength measures the energy required to delaminate a sheet of paper, where fiber fracture is not relevant and increased for X. In addition, fiber-fiber contact increases the fiber-fiber bond strength. Paper density is the simplest and most effective indicator of fiber-fiber contact area and increased for X as is the light scattering coefficient S, which decreases for X. As a result, the addition of xylan increases the fiber network strength by increasing the fiber-fiber bond strength, while the degradation decreases the fiber network strength due to the opposite effects. Similar results were obtained in a study on cellulose nanofibril (CNF) papers, which showed better mechanical performance of the nanopapers containing hemicelluloses as a result of increased bond strength between fibrils with an improvement in specific tensile strength of 35 % compared to nanopapers made from bacterial cellulose (Konturi et al., 2021). Chen et al. (2020) used hemicellulose-rich wood fibers and prepared CNF papers by swelling the hemicelluloses in a mixture of ionic liquid and water to produce a nanonetwork of highly disordered, flexible fibrils that exhibited 240 % higher tensile strength than the water-treated blank. This suggests that the proper distribution of hemicelluloses is important for the network strength and could explain the stronger effect of intrinsic xylan removal compared to extrinsic xylan addition.

## 4. Conclusion

Partial removal of only about 1 % intrinsic xylan from BSKP resulted in a more pronounced fibril structure on the fiber surface, a more permeable, less dense fiber network (i.e. lower sheet density) and inferior mechanical properties. In contrast, the addition of 3 % xylan resulted in a denser fiber network and improved mechanical properties. However, the mechanical properties did not increase to the same extent when extrinsic xylan was added, as they decrease when intrinsic xylan was removed.

These findings support the hypothesis that the improvement of mechanical properties for the xylan adsorbed pulp is caused by a combination of two mechanisms: (i) improvement of fiber-fiber bonds due to an increase in surface fiber charge and increased swelling capacity and (ii) increase in sheet density. Consequently, the decrease in mechanical properties for the enzyme treated pulp is a result of decreased sheet density and a lower bonded area. However, the decrease in mechanical properties is more pronounced than the increase. This suggests that the xylan intrinsically present in the fibers after pulping plays a key role for the tensile strength of the fiber network, which cannot be achieved by simple (re)adsorption of xylan onto pulp fibers. It can be speculated that for the specific conditions in which this study was carried out xylan adsorbs mainly on the surface of the fibers, where it contributes more to the fiber-fiber interactions and thus increases the bonding within the fiber network resulting in denser paper sheets. Moreover, xylan adsorbs in aggregates, which do not contribute as much to the tensile properties. In contrast, the intrinsically present xylan in BSKP might be more incorporated in the inner fiber layers, which is decisive for the tensile strength. The color of the pulp hand sheets is compromised with the adsorption of xylan as white is typically desired over yellow for paper-making applications, hence, indicating an inferior optical performance with extrinsic than with intrinsic xylan.

Although xylan is only a minor constituent of the pulp, significant differences in paper properties are obtained with small variations in xylan content. Hence, paper properties can be adjusted by focusing on the xylan already contained in the pulp. In this study the extrinsic xylan added to the pulp is likely located on the outside of the fibers, where it should be particularly effective in supporting mechanical paper properties, acting as a glue between the fibers. However, the extrinsic (added) xylan was found to be less effective than the intrinsic (present after pulping) xylan. Some xylan has been precipitated on the fibers during pulping, so part of the intrinsic xylan is also located outside the

fiber and hence may contribute to the fiber-fiber bonding.

Based on the observations in this contribution, there may be a benefit in retaining as much intrinsic xylan as possible in the fiber network during pulping and bleaching for better mechanical performance, while extrinsic xylan can be added for better internal bond strength and an increase in sheet density. In contrast, removal of xylan should be aimed for only when a looser fiber network is desired or when brightness is to be increased at the expense of a decrease in tensile strength. In order to support these observations, however, further studies using different pulp grades under varying refining conditions would be of interest.

## Funding

This work has received funding from the European Union's Horizon 2020 research and innovation program under grant agreement No 964430.

## CRediT authorship contribution statement

**Jana B. Schaubeder:** Methodology, Investigation, Validation, Formal analysis, Writing – original draft. **Stefan Spirk:** Conceptualization, Supervision, Writing – review & editing. **Lukas Fliri:** Investigation, Validation, Formal analysis, Writing – original draft. **Eliott Orzan:** Investigation, Validation, Formal analysis, Writing – review & editing. **Veronika Biegler:** Writing – review & editing. **Chonnipa Palasingh:** Investigation, Formal analysis, Writing – review & editing. **Julian Selinger:** Investigation, Formal analysis, Writing – review & editing. **Adelheid Bakhshi:** Methodology, Investigation. **Wolfgang Bauer:** Conceptualization, Writing – review & editing. **Ulrich Hirn:** Conceptualization, Writing – review & editing. **Tiina Nypelö:** Project administration, Funding acquisition, Conceptualization, Writing – review & editing.

## Declaration of competing interest

The authors declare that they have no known competing financial interests or personal relationships that could have appeared to influence the work reported in this paper.

## Data availability

Data will be made available on request.

## Acknowledgement

JS would like to acknowledge Kerstin Roschitz, Bianca Mautner and Irmgard Windisch for their help with the hand sheet forming and characterization and Manuel Eibinger and Harald Plank for helping with the AFM measurements and providing the facilities. TN and EO acknowledge Merima Hasani for access to the HPAEC analysis. GP and TN acknowledge Eero Hiltunen for introduction to zero-span tensile testing. The authors acknowledge the provision of facilities and technical support by Aalto University at OtaNano-Nanomicroscopy Center (Aalto-NMC).

## Appendix A. Supplementary data

Supplementary data to this article can be found online at <https://doi.org/10.1016/j.carbpol.2023.121371>.

## References

- Bajpai, P., Bhardwaj, N. K., Bajpai, P. K., & Jauhari, M. B. (1994). The impact of xylanases on bleaching of eucalyptus kraft pulp. *Journal of Biotechnology*, 38(1), 1–6.
- Bajwa, D. S., Peterson, T., Sharma, N., Shojaeiari, J., & Bajwa, S. G. (2018). A review of densified solid biomass for energy production. *Renewable and Sustainable Energy Reviews*, 96, 296–305.

- Ban, W., & Van Heiningen, A. (2011). Adsorption of hemicellulose extracts from hardwood onto cellulosic fibers. I. Effects of adsorption and optimization factors. *Cellulose Chemistry and Technology*, 45(1), 57.
- Bergnor-Gidner, E. (1998). Influence on pulp quality of conditions during the removal of hexenuronic acids. *Nordic Pulp & Paper Research Journal*, 13(4), 310–316.
- Bhardwaj, N. K., Duong, T. D., & Nguyen, K. L. (2004). Pulp charge determination by different methods: Effect of beating/refining. *Colloids and Surfaces A: Physicochemical and Engineering Aspects*, 236(1), 39–44.
- Biely, P., Singh, S., & Puchart, V. (2016). Towards enzymatic breakdown of complex plant xylan structures: State of the art. *Biotechnology Advances*, 34(7), 1260–1274.
- Buchert, J., Bergnor, E., Lindblad, G., Viikari, L., & Ek, M. (1997). Significance of xylan and glucomannan in the brightness reversion of kraft pulps. *Tappi Journal*, 80(6), 165–171.
- Buchert, J., Teleman, A., Harjunpää, V., Tenkanen, M., Viikari, L., & Vuorinen, T. (1995). Effect of cooking and bleaching on the structure of xylan in conventional pine Kraft pulp. *Tappi Journal*, 78(11), 125–130.
- Busse-Wicher, M., Gomes, T. C. F., Tryfona, T., Nikolovski, N., Stott, K., Grantham, N. J., ... Dupree, P. (2014). The pattern of xylan acetylation suggests xylan may interact with cellulose microfibrils as a twofold helical screw in the secondary plant cell wall of *Arabidopsis thaliana*. *The Plant Journal*, 79(3), 492–506.
- Busse-Wicher, M., Li, A., Silveira, R. L., Pereira, C. S., Tryfona, T., Gomes, T. C. F., ... Dupree, P. (2016). Evolution of xylan substitution patterns in gymnosperms and angiosperms: Implications for xylan interaction with cellulose. *Plant Physiology*, 171(4), 2418–2431.
- Chen, F., Xiang, W., Sawada, D., Bai, L., Hummel, M., Sixta, H., & Budtova, T. (2020). Exploring large ductility in cellulose nanopaper combining high toughness and strength. *ACS Nano*, 14(9), 11150–11159.
- Cheng, K., Sorek, H., Zimmermann, H., Wemmer, D. E., & Pauly, M. (2013). Solution-state 2D NMR spectroscopy of plant cell walls enabled by a dimethylsulfoxide-d<sub>6</sub>/1-Ethyl-3-methylimidazolium acetate solvent. *Analytical Chemistry*, 85(6), 3213–3221.
- Danielsson, S., & Lindström, M. E. (2005). Influence of birch xylan adsorption during kraft cooking on softwood pulp strength. *Nordic Pulp & Paper Research Journal*, 20(4), 436–441.
- Ebringerová, A., & Heinze, T. (2000). Xylan and xylan derivatives – Biopolymers with valuable properties. 1. Naturally occurring xylans structures, isolation procedures and properties. *Macromolecular Rapid Communications*, 21(9), 542–556.
- Eriksson, I., Haglund, L., Lidbrandt, O., & Sahnén, L. (1991). Fiber swelling favoured by lignin softening. *Wood Science and Technology*, 25(2), 135–144.
- Fliri, L., Heise, K., Koso, T., Todorov, A. R., del Cerro, D. R., Hietala, S., ... King, A. W. T. (2023). Solution-state nuclear magnetic resonance spectroscopy of crystalline cellulosic materials using a direct dissolution ionic liquid electrolyte. *Nature Protocols*, 18, 2084–2123.
- Garg, A. P., Roberts, J. C., & McCarthy, A. J. (1998). Bleach boosting effect of cellulase-free xylanase of *Streptomyces thermoviolaceus* and its comparison with two commercial enzyme preparations on Birchwood Kraft pulp. *Enzyme and Microbial Technology*, 22(7), 594–598.
- Han, W., Zhao, C., Elder, T., Chen, K., Yang, R., Kim, D., ... Ragauskas, A. J. (2012). Study on the modification of bleached eucalyptus kraft pulp using birch xylan. *Carbohydrate Polymers*, 88(2), 719–725.
- Henriksson, Å., & Gatenholm, P. (2001). Controlled assembly of glucuronoxylans onto cellulose fibres. *Holzforschung*, 55, 494–502.
- Henriksson, Å., & Gatenholm, P. (2002). Surface properties of CTMP fibers modified with xylans. *Cellulose*, 9(1), 55–64.
- Holding, A. J., Mäkelä, V., Tolonen, L., Sixta, H., Kilpeläinen, I., & King, A. W. T. (2016). Solution-state one- and two-dimensional NMR spectroscopy of high-molecular-weight cellulose. *ChemSusChem*, 9(8), 880–892.
- Hu, G., Fu, S., Liu, H., & Lucia, L. A. (2016). The role of absorbed hemicelluloses on final paper properties and printability. *Fibers and Polymers*, 17(3), 389–395.
- Jacobs, A., & Dahlman, O. (2001). Characterization of the molar masses of hemicelluloses from wood and pulps employing size exclusion chromatography and matrix-assisted laser desorption ionization time-of-flight mass spectrometry. *Biomacromolecules*, 2(3), 894–905.
- Johansson, M. H., & Samuelson, O. (1977). Alkaline destruction of birch xylan in the light of recent investigations of its structure. *Svensk Papperstidning*, 80(16), 519–524.
- Kabel, M. A., van den Borne, H., Vincken, J.-P., Voragen, A. G. J., & Schols, H. A. (2007). Structural differences of xylans affect their interaction with cellulose. *Carbohydrate Polymers*, 69(1), 94–105.
- Kes, M., & Christensen, B. E. (2013). A re-investigation of the Mark–Houwink–Sakurada parameters for cellulose in Cuen: A study based on size-exclusion chromatography combined with multi-angle light scattering and viscometry. *Journal of Chromatography A*, 1281, 32–37.
- King, A. W. T., Mäkelä, V., Kedzior, S. A., Laaksonen, T., Partl, G. J., Heikkinen, S., ... Kilpeläinen, I. (2018). Liquid-state NMR analysis of nanocelluloses. *Biomacromolecules*, 19(7), 2708–2720.
- Köhnke, T., Lund, K., Breid, H., & Westman, G. (2010). Kraft pulp hornification: A closer look at the preventive effect gained by glucuronoxylan adsorption. *Carbohydrate Polymers*, 81(2), 226–233.
- Kontturi, K. S., Lee, K.-Y., Jones, M. P., Sampson, W. W., Bismarck, A., & Kontturi, E. (2021). Influence of biological origin on the tensile properties of cellulose nanopapers. *Cellulose*, 28(10), 6619–6628.
- Koso, T., Rico del Cerro, D., Heikkinen, S., Nypelö, T., Buffiere, J., Perea-Buceta, J. E., ... King, A. W. T. (2020). 2D assignment and quantitative analysis of cellulose and oxidized celluloses using solution-state NMR spectroscopy. *Cellulose*, 27(14), 7929–7953.

- Laine, J., Hynynen, R., & Stenius, P. (1997). *The effect of surface chemical composition and charge on the fibre and paper properties of unbleached and bleached kraft pulps* (pp. 859–892). Pira International.
- Linder, Å., Bergman, R., Bodin, A., & Gatenholm, P. (2003). Mechanism of assembly of xylan onto cellulose surfaces. *Langmuir*, 19, 5072–5077.
- Linder, Å., & Gatenholm, P. (2003). Effect of cellulose substrate on assembly of Xylans. In *Hemicelluloses: Science and technology* (pp. 236–253). American Chemical Society.
- Mandlez, D., Koller, S., Eckhart, R., Kulachenko, A., Bauer, W., & Hirn, U. (2022). Quantifying the contribution of fines production during refining to the resulting paper strength. *Cellulose*, 29(16), 8811–8826.
- Miletzky, A., Fischer, W. J., Czibula, C., Teichert, C., Bauer, W., & Schennach, R. (2015). How xylan effects the breaking load of individual fiber–fiber joints and the single fiber tensile strength. *Cellulose*, 22(1), 849–859.
- Motamedian, H. R., Halilovic, A. E., & Kulachenko, A. (2019). Mechanisms of strength and stiffness improvement of paper after PFI refining with a focus on the effect of fines. *Cellulose*, 26(6), 4099–4124.
- Paës, G., Berrin, J.-G., & Beaugrand, J. (2012). GH11 xylanases: Structure/function/properties relationships and applications. *Biotechnology Advances*, 30(3), 564–592.
- Palasingh, C., Nakayama, K., Abik, F., Mikkonen, K. S., Evenäs, L., Ström, A., & Nypelö, T. (2022). Modification of xylan via an oxidation–reduction reaction. *Carbohydrate Polymers*, 292, Article 119660.
- Pawar, P., Koutaniemi, S., Tenkanen, M., & Mellerowicz, E. (2013). Acetylation of woody lignocellulose: Significance and regulation. *Frontiers in Plant Science*, 4, 118.
- Pettersson, S. E., & Rydholm, S. A. (1961). Hemicelluloses and paper properties of birch pulps, part 3. *Svensk Papperstidning*, 64(1), 4–17.
- Przybysz Buzala, K., Kalinowska, H., Borkowski, J., & Przybysz, P. (2018). Effect of xylanases on refining process and kraft pulp properties. *Cellulose*, 25(2), 1319–1328.
- Pulkkinen, I., Ala-Kaila, K., & Aittamaa, J. (2006). Characterization of wood fibers using fiber property distributions. *Chemical Engineering and Processing: Process Intensification*, 45(7), 546–554.
- Qaseem, M. F., & Wu, A.-M. (2020). Balanced xylan acetylation is the key regulator of plant growth and development, and cell wall structure and for industrial utilization. *International Journal of Molecular Sciences*, 21(21), 7875.
- Rodell Lundgren, K., Bergkvist, L., Högman, S., Jöves, H., Eriksson, G., Bartfai, T., van der Laan, J., Rosenberg, E., & Shoham, Y. (1994). TCF mill trial on softwood pulp with Korsäs thermostable and alkaline stable xylanase T6. *FEMS Microbiology Reviews*, 13, 365–368.
- Rohm, S., Hirn, U., Ganser, C., Teichert, C., & Schennach, R. (2014). Thin cellulose films as a model system for paper fibre bonds. *Cellulose*, 21(1), 237–249.
- Roncero, M. B., Torres, A. L., Colom, J. F., & Vidal, T. (2003). TCF bleaching of wheat straw pulp using ozone and xylanase. Part A: Paper quality assessment. *Bioresource Technology*, 87(3), 305–314.
- Rydholm, S. A. (1965). *Pulping process interscience publishers* (pp. 1–1231). New York-London-Sydney: Jeam Wiley S. Sons. Inc..
- Schönberg, C., Oksanen, T., Suurnäkki, A., Kettunen, H., & Buchert, J. (2001). The importance of Xylan for the strength properties of spruce Kraft pulp Fibres. *Holzforchung*, 55(6), 639–644.
- Shimizu, K. (1991). *Chemistry of hemicelluloses* (2 ed.). New York - Basel: Marcel Dekker, Inc.
- Silva, J. C.d., Oliveira, R. C.d., Neto, A.d. S., Pimentel, V. C., & Santos, A.d. A.d. (2015). Extraction, addition and characterization of hemicelluloses from corn cobs to development of paper properties. *Procedia Materials Science*, 8, 793–801.
- Sjöberg, J., Kleen, M., Dahlman, O., Agnemo, R., Ab, D. F., & Sundvall, H. (2004). Fiber surface composition and its relations to papermaking properties of soda-anthraquinone and kraft pulps. *Nordic Pulp & Paper Research Journal*, 19(3), 392–396.
- Suurnäkki, A., Heijnesson, A., Buchert, J., Tenkanen, M., Viikari, L., & Westermark, U. (1996). Location of xylanase and mannanase action in kraft fibres. *Journal of Pulp and Paper Science*, 22(3), 78–83.
- Theander, O., & Westerlund, E. A. (1986). Studies on dietary fiber. 3. Improved procedures for analysis of dietary fiber. *Journal of Agricultural and Food Chemistry*, 34(2), 330–336.
- Wierzbicki, M. P., Maloney, V., Mizrachi, E., & Myburg, A. A. (2019). Xylan in the middle: Understanding xylan biosynthesis and its metabolic dependencies toward improving wood fiber for industrial processing. *Frontiers in Plant Science*, 10, 176.
- Wojtasz-Mucha, J., Hasani, M., & Theliander, H. (2017). Hydrothermal pretreatment of wood by mild steam explosion and hot water extraction. *Bioresource Technology*, 241, 120–126.